2009

Development of an Electroencephalography-Based Brain-Computer Interface Supporting Two-Dimensional Cursor Control

Dandan Huang
Virginia Commonwealth University

School of Engineering
Virginia Commonwealth University

This is to certify that the thesis prepared by Dandan Huang entitled "Development of an Electroencephalography-Based Brain-Computer Interface Supporting Two-Dimensional Cursor Control" has been approved by her committee as satisfactory completion of the thesis requirement for the degree of Master of Science.

Ding-Yu Fei, Ph.D., Director of Thesis, School of Engineering

Ou Bai, Ph.D., School of Engineering

Azhar Rafiq, Ph.D., School of Medicine

Gerald Miller, Ph.D., Chair, Department of Biomedical Engineering, School of Engineering

Rosalyn Hobson, Ph.D., Associate Dean of Graduate Studies, School of Engineering

Russell Jamison, Ph.D., Dean, School of Engineering

F. Douglas Boudinot, Ph.D., Dean of the Graduate School

Date

DEVELOPMENT OF AN ELECROENCEPHALOGRAPHY-BASED BRAIN-

COMPUTER INTERFACE SUPPORTING TWO-DIMENSIONAL CURSOR

CONTROL

A thesis submitted in partial fulfillment of the requirements for the degree of Master of Science at Virginia Commonwealth University.

by

DANDAN HUANG
B.S., Tianjin University, People's Republic of China, 2007

Director: DING-YU FEI, PH.D.
Associate Professor, Department of Biomedical Engineering

Virginia Commonwealth University
Richmond, Virginia
August, 2009

Acknowledgments

I would like to express my gratitude to all the people who have given their heart whelming full support in making this project a magnificent experience. Special thanks are given to my parents, my directors Dr. Ding-Yu Fei and Dr. Ou Bai. They inspired, encouraged, and fully supported me for every trial that came on my way, not just financially, but also morally and spiritually. I also would like to thank my committee member Dr. Azhar Rafiq for his thoughtful comments and helpful discussion, thank Ms. Cai-Ting Fu and thank my group mates who willingly helped me gather the experimental data and information for the project.

Table of Contents

List of Abbreviations

ALS	Amyotrophic Lateral Sclerosis
ANOVA	One-way Analysis of Variance
BCI	Brain-Computer Interface
CNS	Central Nervous System
DTC	Decision Tree Classifier
ECoG	Electrocorticography
EEG	Electroencephalography
EMG	Electromyography
EOG	Electrooculogram
ERD	Event-Related Desynchronization
ERS	Event-Related Synchronization
FFT	Fast Fourier Transform
fMRI	Functional Magnetic Resonance Imaging
GA	Genetic Algorithm
GA-MLD	Genetic Algorithm Based Mahalanobis Linear Distance
GUI	Graphical User Interface
ITR	Information Transfer Rate
LFP	Local Field Potentials
MEG	Magnetoencephalography
MLD	Mahalanobis Linear Discriminator

NIRS	Near-Infrared Signal
PSD	Power Spectrum Density
QOL	Quality Of Life
SLD	Surface Laplacian Derivation
SVM	Support Vector Machine

List of Tables

List of Figures

Abstract

DEVELOPMENT OF AN ELECTROENCEPHALOGRAPHY-BASED BRAIN-COMPUTER INTERFACE SUPPORTING TWO-DIMENSIONAL CURSOR CONTROL

By Dandan Huang, M. S.

A thesis submitted in partial fulfillment of the requirements for the degree of Master of Science at Virginia Commonwealth University.

Virginia Commonwealth University, 2009

Major Director: Ding-Yu Fei, Ph.D.
Associate Professor, Department of Biomedical Engineering

This study aims to explore whether human intentions to move or cease to move right and left hands can be decoded from spatiotemporal features in non-invasive electroencephalography (EEG) in order to control a discrete two-dimensional cursor movement for a potential multi-dimensional Brain-Computer interface (BCI). Five naïve subjects performed either sustaining or stopping a motor task with time locking to a

predefined time window by using motor execution with physical movement or motor imagery. Spatial filtering, temporal filtering, feature selection and classification methods were explored. The performance of the proposed BCI was evaluated by both offline classification and online two-dimensional cursor control. Event-related desynchronization (ERD) and post-movement event-related synchronization (ERS) were observed on the contralateral hemisphere to the hand moved for both motor execution and motor imagery. Feature analysis showed that EEG beta band activity in the contralateral hemisphere over the motor cortex provided the best detection of either sustained or ceased movement of the right or left hand. The offline classification of four motor tasks (sustain or cease to move right or left hand) provided 10-fold cross-validation accuracy as high as 88% for motor execution and 73% for motor imagery. The subjects participating in experiments with physical movement were able to complete the online game with motor execution at the average accuracy of 85.5±4.65%; Subjects participating in motor imagery study also completed the game successfully. The proposed BCI provides a new practical multi-dimensional method by noninvasive EEG signal associated with human natural behavior, which does not need long-term training.

CHAPTER 1

Introduction

1.1 Background

For many years people have speculated that electroencephalographic activity or other electrophysiological measures of brain function might provide a new non-muscular channel for sending messages and commands to the external world – a brain–computer interface (BCI) [1], which is a direct communication pathway between a brain and an external device. Research on BCIs began in 1970s at the University of California Los Angeles (UCLA). The field has since blossomed spectacularly, mostly toward neuroprosthetics applications that aim at restoring damaged hearing, sight and movement. Over the past 15 years, productive BCI research programs have arisen. Encouraged by new understanding of brain function, by the advent of powerful low-cost computer equipment, and by growing recognition of the needs and potentials of people with disabilities, these programs have concentrated on developing new augmentative communication and control technologies for those with severe neuromuscular disorders, such as amyotrophic lateral sclerosis, brainstem stroke, and spinal cord injury [1, 2]. The immediate goal is to provide these users, who may be completely paralyzed, or 'locked in', with basic communication

capabilities so that they can express their wishes to caregivers or even operate word processing programs or neuroprostheses [3]. Current BCIs determine the intent of the user from a variety of different electrophysiological signals. These signals include slow cortical potentials, P300 potentials, and mu or beta rhythms recorded from the scalp, and cortical neuronal activity recorded by implanted electrodes [4-6]. They are translated in real-time into commands that operate a computer display or other device. Successful operation requires that the user encodes commands in these signals and then the BCI derives the commands from the signals. Thus, the user and the BCI system need to adapt to each other both initially and continually so as to ensure stable performance [1]. Current BCIs have maximum information transfer rates up to 10–25 bits/min[1, 7]. This limited capacity can be valuable for people whose severe disabilities prevent them from using conventional augmentative communication methods. At the same time, many possible applications of BCI technology, such as neuroprosthesis control, may require higher information transfer rates [1, 8].

Current BCIs use a variety of invasive and non-invasive methods to record brain signals and a variety of signal processing methods. Whatever recording and processing methods are used, BCI performance (e.g. the ability of a BCI to control movement of a computer cursor) is highly variable and, by the standards applied to neuromuscular control, could be described as ataxic. In the effort to understand this imperfection, two principles can be used to help underlie the brain's normal motor outputs. The first principle is that motor outputs are normally produced by the combined activity of many central nervous system (CNS) areas, from the cortex to the spinal cord [9]. Together, these areas produce

2

appropriate control of the spinal motor neurons that activate muscles. The second principle is that the acquisition and life-long preservation of motor skills depend on continual adaptive plasticity throughout the CNS [10]. This plasticity optimizes the control of spinal motor neurons. In the light of these two principles, a BCI may be viewed as a system that changes the outcome of CNS activity from control of spinal motor neurons to control of the cortical (or other) area. The signals from the cortical area are used by the BCI to determine the user's intent. In essence, a BCI attempts to assign to cortical neurons the role normally performed by spinal motor neurons. Thus, a BCI requires that the many CNS areas involved in producing normal motor actions change their roles so as to optimize the control of cortical neurons rather than spinal motor neurons. The disconcerting variability of BCI performance may stem in large part from the challenge presented by the need for this unnatural adaptation. This difficulty might be reduced, and BCI development might thereby benefit, by adopting a 'goal-selection' rather than a 'process-control' strategy. Not only is 'goal selection' less demanding, but also, by delegating lower-level aspects of motor control to another structure (rather than requiring that the cortex do everything), it more closely resembles the distributed operation characteristic of normal motor control.

1.2 Literature review

1.2.1 Brain-computer interface

The brain-computer interface (BCI) provides a new means of direct brain communication with the external environment for patients who may partly or entirely lose voluntary muscle contraction such as in the 'locked-in' state [3]. Such patients lost control

of their motor faculties, and can no longer outwardly express their needs and thoughts. These kinds of disorders have a significant effect on the quality of life (QOL) for both patients themselves and their families [11]. A potential solution is to provide the brain with a new, non-muscular communication and control channel, a direct brain-computer interface (BCI) for conveying messages and commands to the external world [1]. A BCI enables these "locked in" patients to control a computer with their brain activity for communication, mobility, and other purposes. Among the different techniques for decoding human brain signals for BCI communication, there are invasive methods using neuronal spikes [12] or local field potentials (LFP) [13], non-invasive methods using electroencephalography (EEG) [14], magnetoencephalography (MEG) [15], functional magnetic resonance imaging (fMRI) [16] or near-infrared signal (NIRS) [17], [18] and the invasive method of electrocorticography (ECoG) [19]. Although some invasive methods have achieved scientific success in terms of high-speed communication and possible multidimensional control [20],[21],[22] in non human primate studies, these methods are still far from practical clinical applications because of technical difficulties such as the need for chronic recordings and, in particular, the balance between benefit and risk due to required surgical implantation of the electrodes. Furthermore, as invasive methods have been investigated mainly in intact non-human primates, there is a large gap for the clinical applications as BCI designed for paralyzed or "locked-in" human patients [23]. Among non-invasive methods, only EEG and related methods, which have relatively short time constants, can function in most environments and require relatively simple and inexpensive equipment, offering the realistic possibility for patients to use their brain signals to directly

4

control external devices[11]. Several successful EEG-based BCI methods have been reported: a slow cortical potential-based thought translation device [4], Mu rhythm-based cursor control [5] and P300-based letter selection [6]. For the P300-based BCI, the communication accuracy may decrease significantly with time due to easy fatigue [24]. Both slow cortical potential and Mu rhythm control methods require long-term training before subjects can attain robust communication or control [25]. This significantly limits the clinical application of BCI since many patients with severe neurological disorders have difficulty tolerating long-term training [26], in particular those with 'locked-in' syndrome.

One of the most useful applications for BCI is to control an external device, e.g. wheelchair or robotic arms, to restore motor function [27]. This purpose requires a BCI capable of multidimensional control. Although multidimensional control is highly promising using invasive methods, e.g. local field potentials/spike train [21, 28], or semi-invasive methods using electrocorticography (ECoG) [19], the noninvasive methods, in particular, electroencephalography (EEG), mainly support one dimensional control [29, 30]. Successful two-dimensional BCI using noninvasive EEG signals has been achieved [25]. However, subjects needed long-term training, up to several months, before they could reliably attain two-dimensional BCI control.

Recent studies have developed a scheme to achieve two-dimensional control by sequentially combining two binary controls [31, 32]. Though sequential combination of one-dimensional control may achieve two-dimensional control, direct two-dimensional control, i.e. simultaneous control of four directions in a two-dimensional plane, will be more effective, and thus, more convenient for use.

5

1.2.2 Even-related oscillations

Human somatotopic organization indicates that human limbs are controlled by contralateral brain hemispheres. Many neurophysiological and neuroimaging studies have confirmed the nature of contralateral control [33-35]. Therefore, reliably decoding the movement intention of right and left hand, which are associated with different spatiotemporal patterns of event-related desynchronization (ERD), i.e. oscillation amplitude attenuation, and event-related synchronization (ERS), i.e. oscillation amplitude increase, may provide additional degrees-of-freedom for control. During physical and motor imagery of right and left hand movements, beta band brain activation (15-30 Hz) ERD occurs predominantly over the contralateral left and right motor areas. The brain activity associated with ceasing to move, the post movement ERS, can also be found over the contralateral motor areas. It suggests that the brain activity associated with four natural motor behaviors (thus, not requiring training) may potentially provide four reliable features for a discrete two-dimensional control, e.g. left-hand ERD to command move to the left, left-hand ERS to command move up, right-hand ERD to command move to the right, and right-hand ERS to command move down. As the spatial distribution of post movement beta rebound (ERS) is more focal than ERD distribution, the detection of ERS might be potentially more reliable than ERD detection only [36]. As a result, the proposed method to discriminate spatial distribution of ERD and ERS might provide more accurate classification than previous methods relying on the detection of ERD only [37, 38].

6

Although evidence has demonstrated separate spatial patterns of ERD and ERS with physical movement, it is also important to know about the hemispheric patterns during motor imagery of limb movement which is essential for achieving purely mental control without involvement of muscle activity.

1.3 Objective of this study

In summary, the aim of this study is to introduce a novel BCI paradigm/method: decoding ERD and ERS associated with natural motor behavior so that the subjects can control cursor movement in a two-dimensional plane with minimal training. We have tested whether the decoding of multiple movement intentions is reliable enough to control a two-dimensional computer cursor for a possible multi-dimensional brain-computer interface (BCI). We also employed advanced signal processing and classification methods for better decoding of human intentions from single trial EEG to improve the performance of the proposed BCI paradigm. The reliability of two-dimensional cursor control has been tested on a virtual online computer game.

CHAPTER 2

Experimental Design

2.1 System Description

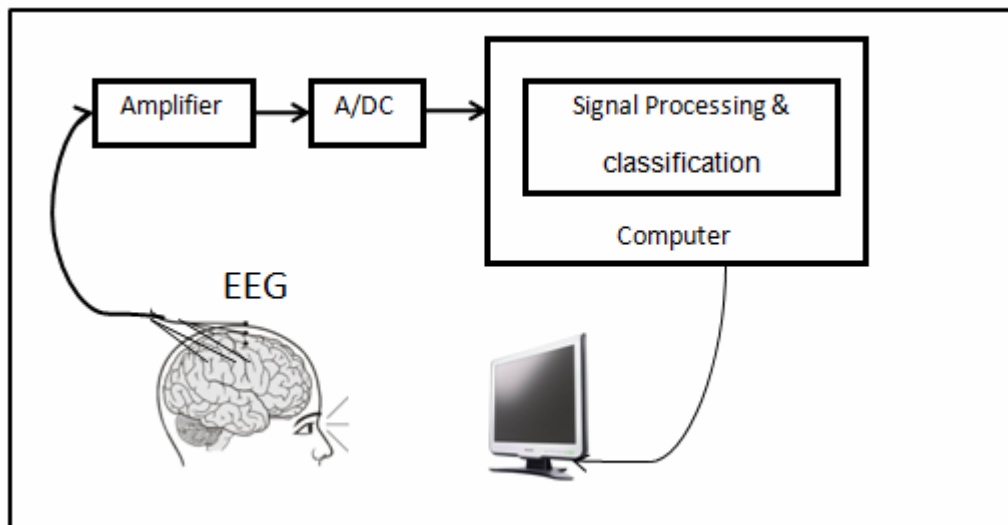**Figure 1. Experimental system. EEG signals were picked up from scalp and amplified, then were digitized through A/D convertor and sent to the computer for signal processing.**

Figure 1 shows the system setup. A monitor was placed in front of the subject, presenting the experimental paradigm. Meanwhile, EEG signal was recorded from 27 (tin) surface electrodes attached on an elastic cap. Surface electromyography (EMG), which

was used to monitor the movement and bipolar electrooculogram (EOG) above left eye and below right eye were also recorded. The analog signals were amplified, and then digitized through A/D convertor. The digital signal was then sent to a computer for online processing.

2.2 Subject

Five healthy volunteers (three females and two males) between the ages of 20 and 27 participated in this study. They were right-handed according to the Edinburgh inventory [39]. All subjects gave informed consent. Prior to this study, none of these subjects had been exposed to a BCI system or were informed of the experimental hypothesis. The protocol was approved by the Institutional Review Board.

2.3 Experimental paradigm

The experimental paradigm in this study was similar to a previous study [32], including two sessions. The first session was motor execution with physical movement, and all five subjects participated in. The second session was motor imagery, and two (S1 and S2) of the five subjects were also available to further participate in the second session.

During the recording, a quiet environment with dim light was provided to maintain the subjects' attention level. Subjects were seated in a chair with the forearms semi-flexed and supported by a pillow. They were asked to keep all muscles relaxed, except for those in the performing arms; besides, they were also instructed to avoid eye movements, blinks, body adjustments, swallowing or other movements during the visual cue onset. During motor imagery, the investigator monitored the EMG activity continuously; once EMG activity

was observed, subjects were reminded to relax the muscles. Trials with EMG contamination were excluded based on visual inspection for further offline ERD and ERS feature analysis and classification. Each of the motor execution with physical movement and motor imagery sessions contained an initial calibration step to determine the optimal frequency band and spatial channels. The selected features and generated model were then used to test an online two-dimensional-cursor-control game. The two sessions were performed continuously within three to four hours in a single visit.

2.3.1 Calibration

Visual stimuli were periodically presented on a computer screen, placed in front of the subjects, with the distance and the height adjusted for subject's comfort. In the first session (pure physical movement), there were four cues in the task paradigm, 'RYes', 'RNo', 'LYes', and 'LNo' ('R' indicating right hand task, and 'L' for left hand task). The visual cue was displayed for a period of T1 in green color, followed by a color change of the cue to blue, which was illustrated in Figure 2. The second cue was displayed for a period of T2, after which the cue disappeared. The lengths of T1 and T2 window were set to 2.5 s initially. The time interval between the end of T2 and the next T1, i.e. trial-to-trial interval, was set to 2 seconds. Subjects were instructed to begin repetitive wrist extensions of the right arm at the onset of the initial cue 'RYes' or 'RNo'. At the time of color change, the subject was instructed to continue movement with the 'Yes' cue or abruptly relax and stop

moving with the 'No' cue. The task was similar for 'LYes' and 'LNo', where subjects performed left hand instead.

In the calibration step for motor imagery, subjects were asked to perform both physical movement and motor imagery according to eight cues: 'PHYRYes', 'PHYRNo', 'PHYLYes', 'PHYLNo' (for physical movement) and 'MIRYes', 'MIRNo', 'MILYes', 'MILNo' (for motor imagery). The alternation of physical movement and motor imagery was intended to provide the subject with a vivid mental sensation of physical movement for better motor imagery. The visual cues were randomly presented, and the subject performed either physical movement or motor imagery, using either right or left hand, following the instruction of the ongoing cue. The lengths of T1 and T2 were adjusted according to the different response delays for each subject, and kept consistent in the following sessions/steps.

The calibration procedure for the physical movement session consisted of three or four blocks of trials, each block consisting of 48 trials, 24 'Yes' or 'No' stimuli with total duration of 6-7 min. The 'Yes' and 'No' stimuli were provided pseudo-randomly. The calibration for the motor imagery session consisted of two to four blocks of trials, each block consisting of 96 trials, with 'PHY' and 'MI' appearing pseudo-randomly for alternating physical movement and motor imagery, and 48 'Yes' and 48 'No' stimuli with total duration of 12-13 min.
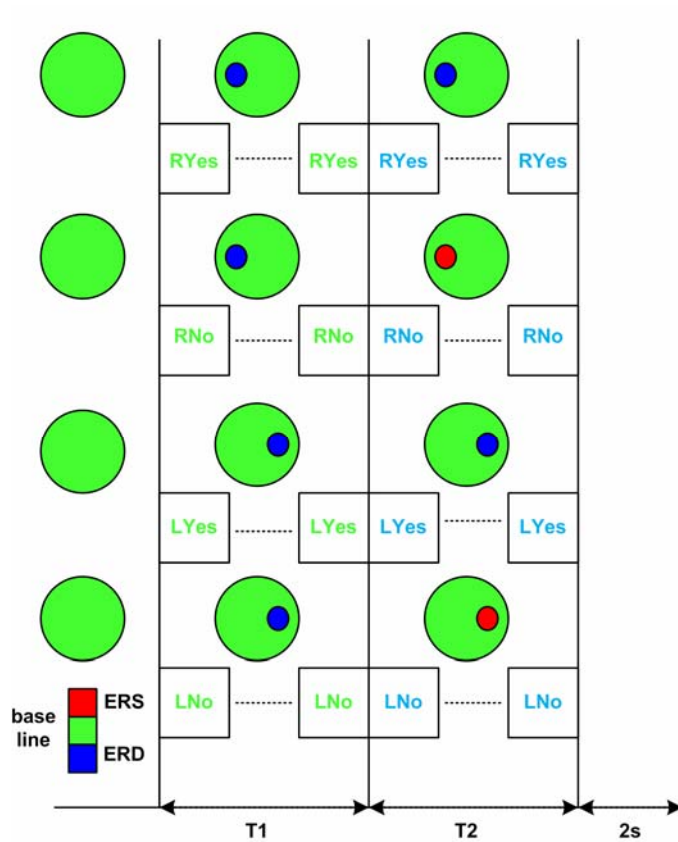
Figure 2. Calibration paradigm. In the case of 'RYes', subjects were instructed to start motor execution or motor imagery with right hand when the first cue presented (green color) at the beginning of T1 window; when the color of cue turned to blue at the beginning of T2 window, subjects were instructed to sustain motor execution or motor imagery (ERD indicating with small blue circle was expected on the left hemisphere, see detail in the text) In the case of 'RNo' with right hand, subjects were instructed to start motor execution or motor imagery when the first cue presented (green color) at the beginning of T1 window; when the color of cue turned to blue at the beginning of T2 window, subjects were instructed to stop motor execution or motor imagery (ERS by small red circle was expected on the left hemisphere). Procedures were similar for 'LYes' and 'LNo' with left hand motor execution or motor imagery.

12

2.3.2 Discrete Two-dimensional-cursor-control game

Sustained physical movement is usually associated with a persistent event-related desynchronization (ERD), while cessation of movement is followed by a beta band rebound above baseline power levels, i.e. event-related synchronization (ERS). Since we intended to discriminate ERD from ERS, which occurs only after cessation of movement in the T2 window, we only extracted EEG signal in the T2 time window to classify 'Yes' or 'No' intention determined from ERD and ERS. Successfully classifying the four kinds of movements in motor execution or motor imagery was the basis of realization of 2D control.

In a 2D plane, the cursor can move to four directions: up, down, right and left, each of which was linked to one of the four movements. We intended to decode movement intentions to determine the subject's control of cursor direction. As human movement intention is associated with spatial ERD and ERS (on either left or right hemisphere), we applied the detection strategy as shown in Figure 3. For example, if the subject wanted to move the cursor to the right, he needed to perform the 'RYes' task, either physical or motor imagery to develop an ERD pattern on the right hemisphere. When the associated ERD on the left hemisphere was detected in the T2 time window, the cursor would move to the right direction; similarly, if the subject wanted to move the cursor upward, he needed to perform the 'LNo' task, and when the associated ERS on the right hemisphere was detected in T2 window, the cursor would move upward accordingly.
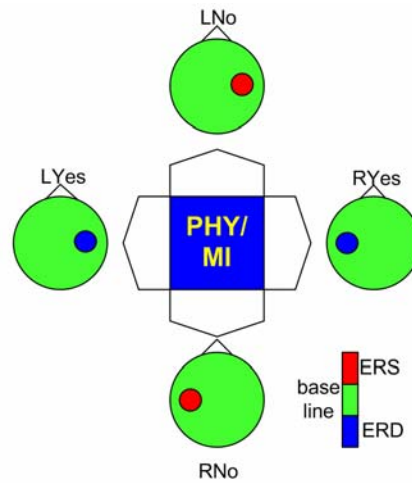
Figure 3. Scheme of 2D cursor control. Four directions control by spatial detection of ERD/ERS on right/left hemisphere associated with intention to move or cease to move of left/right hand. In order to control cursor moving to left ('LYes' direction), subjects may perform sustained physical movement/motor imagery so that ERD on the right hemisphere can be detected. It is similar for other direction controls.

Upon successfully decoding movement intentions in the offline analysis, the subjects played a game of two-dimensional control of cursor movement on a computer monitor. A brief description of the 2D cursor-control game is given here since the detailed design of the online game was similar to the one given for binary cursor-control game [32]. Subjects were instructed to move the cursor to the target and avoid a designated 'trap'. Cues were presented with the same duration as that in the calibration session. Classification of 'Yes' and 'No' trials of right and left hands were used to direct 2D control correlated with cursor movement. As illustrated in Figure 3, the detection of 'LYes' will direct the cursor move to the left, and similar with the other directions. The initial positions of cursor, target and trap

were provided pseudo-randomly and the number of detections was different in each game. Subjects played 4-6 games and they were allowed 5-10 min to practice the game before the test.

In the online 2D game, subjects determined the path to reach the target using their own game strategy. From the example shown in Figure 4(a), the subject may choose to move to the right instead of downward in that situation. It was also possible that the subject would choose to move up to the margin of the grid and then move along the margin to the target. Due to the various strategies, it was difficult to determine the cursor-control accuracy from the path of the cursor movement. Instead, in the case of physical movement, we used the EMG activity in the detection window to interpret whether the subjects desired to move to one of four directions, and as a result, the control accuracy could be quantitatively determined from the actual cursor movement from the EEG derived results. In the case of motor imagery for online game, the subjects determined the direction to move; as there was no EMG activity of motor imagery, we were unable to know whether each movement was correctly decoded as the subject intended. Therefore, instead of quantitative measurement of control accuracy, we qualitatively evaluated the success of the two-dimensional cursor control with motor imagery by whether the subjects could control the cursor to reach the target. However, if the cursor was moved into the trap or the total number of moves reached the limit of 5 times of the possible shortest moves, the game would automatically stop. We considered the successful judgment of the two-dimensional cursor control with motor imagery to be a qualitative measurement. The quantitative measurements of control accuracy for motor imagery were determined from the visually-

15

cued motor imagery of wrist extension, i.e. in the calibration procedure. Figure 5 gives an example of successfully controlled 2D game.
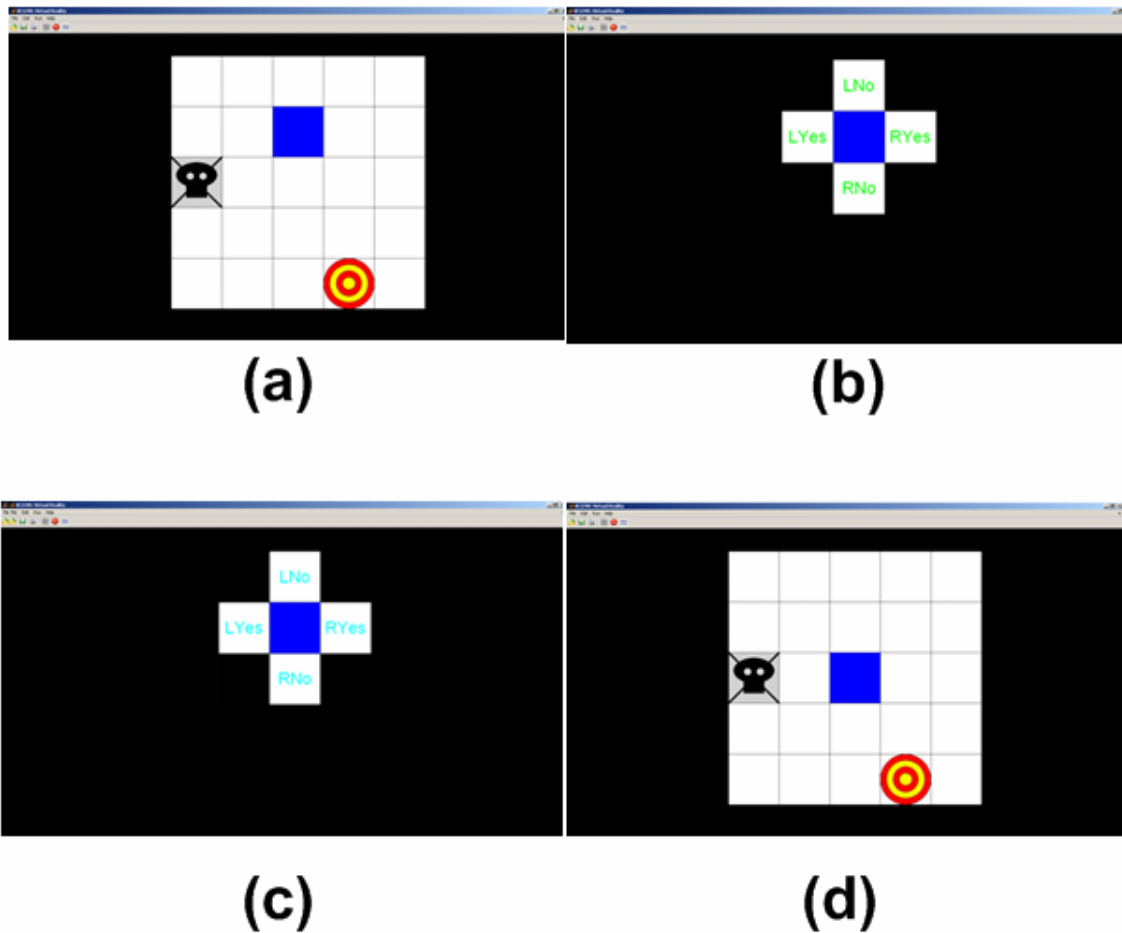
Figure 4. Paradigm of discrete two-dimensional cursor-control game. (a) A game grid is displayed for 2-3 s showing a cursor (blue), target (red) and trap (black). (b) All squares except those adjacent to the cursor are masked and green prompts are displayed in the adjacent squares. (c) After a T1 delay, these prompts turn blue and remain for a period of T2. (d) The subject's response uniquely determines the cursor movement direction, which the cursor slides to. The entire process (a)-(d) then repeats for the next cursor move, and so on until the target is obtained, the trap is hit or too many moves have been made.
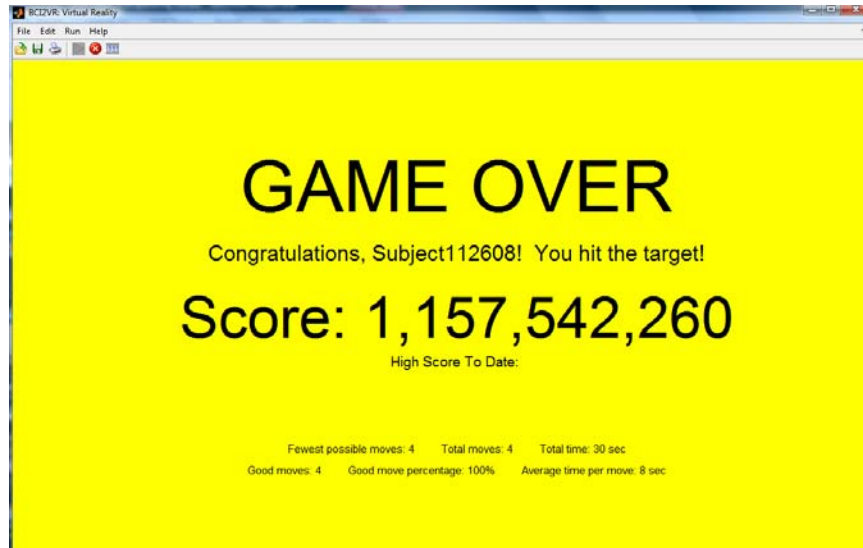
Figure 5. Result of a 2D game given by BCI2VR Virtual Reality. This picture shows the subject completed the game by hitting the target.

The main purpose for the proposed computer game was to improve the subjects' motivation in participating in the investigation. The subjects played the game with physical movements first. When the subjects were comfortable with the game, whether the subjects could play the game with motor imagery was determined.

2.3.3 Mental strategy for motor imagery

In motor imagery part, the subjects were asked to imagine repetitive wrist extension of their own hands. As motor imagery is not a routine natural behavior in daily life, usually mental training with feedback is required before the subjects can perform vivid imagination of the movement [40]. In this study, there was no feedback in the calibration procedure for motor imagery and the modeling under the calibration data may be

unreliable if subjects were unable to make imagination of physical movements. In order to achieve better calibration as well as modeling, subjects performed both physical movement and motor imagery in the calibration step in motor imagery session. Our assumption was that subjects would be able to imagine more vividly right after a physical movement. However, only the data associated with motor imagery were used for offline calibration and modeling for the subsequent motor imagery study. In motor imagery task, subjects reported difficulty with imagining the termination of movement. We guided them to stop imagining movement by switching from the imagination of motor task to a non-motor task such as reciting the alphabet or counting numbers mentally.

CHAPTER 3

Data Acquisition and Online Processing System

EEG was recorded from 27 (tin) surface electrodes (F3, F7, C3A(PC3), C1, C3, C5, T3, C3P(CP3), P3, T5(P7), F4, F8, C4A(PC4), C2, C4, C6, T4, C4P(CP4), P4, T6, FPZ, FZ, FCZ(PCZ), CZ, CZP(CPZ), PZ and OZ) attached on an elastic cap (Electro-Cap International, Inc., Eaton, OH, U.S.A.) according to the international 10-20 system [41], with reference from the right ear lobe and ground from the forehead. Figure 6 shows the placement of the 27 electrodes (marked by red circles) on the cap. For surface electromyography (EMG), which was used to monitor the movement, two electrodes were filled with conductive gel and taped over the right and left wrist extensors. Electrodes for bipolar electrooculogram (EOG) above left eye and below right eye were also pasted.

Total duration of preparation included time to obtain informed consent, paradigm explanation, setting up the electrodes and preparations of hardware and software. This procedure took about 30 min to 1 hour. Signals from all the channels were amplified using a 64 channel g.USBamp-System (g.tec GmgH, Schiedlberg, Austria), filtered (0.1-100 Hz) and digitized (sampling frequency was 250 Hz) through A/D convertor.
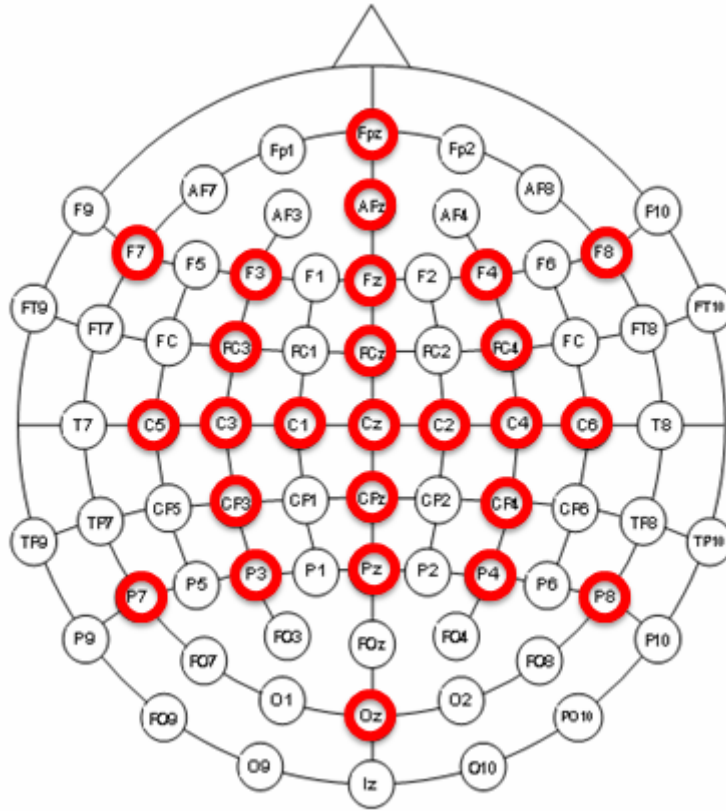
Figure 6. Placement of 27 electrodes on the cap, circled by red. They are F3, F7, PC3 (C3A), C1, C3, C5, T3, CP3 (C3P), P3, P7 (T5), F4, F8, PC4 (C4A), C2, C4, C6, T4, CP4 (C4P), P4, T6, FPZ, FZ, PCZ (FCZ), CZ, CPZ (CZP), PZ and OZ

The digital signals were then sent to a HP PC workstation and were online processed using a home-made MATLAB (MathWorks, Natick, MA) Toolbox: brain-computer interface to virtual reality or BCI2VR [31, 32] (Figure 7 shows the Graphical User Interface (GUI) of BCI2VR). The BCI2VR programs provided both the visual stimulus for the calibration and the two-dimensional cursor-control game, as well as online processing of the EEG signal (showing by Figure 8). The signal for decoding was extracted following the cues from the visual stimulus.

20
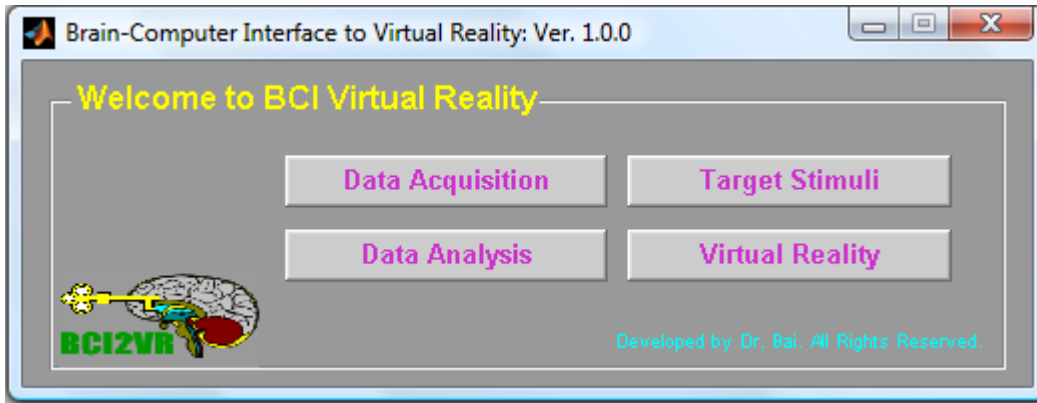
Figure 7. BCI2VR GUI interface.
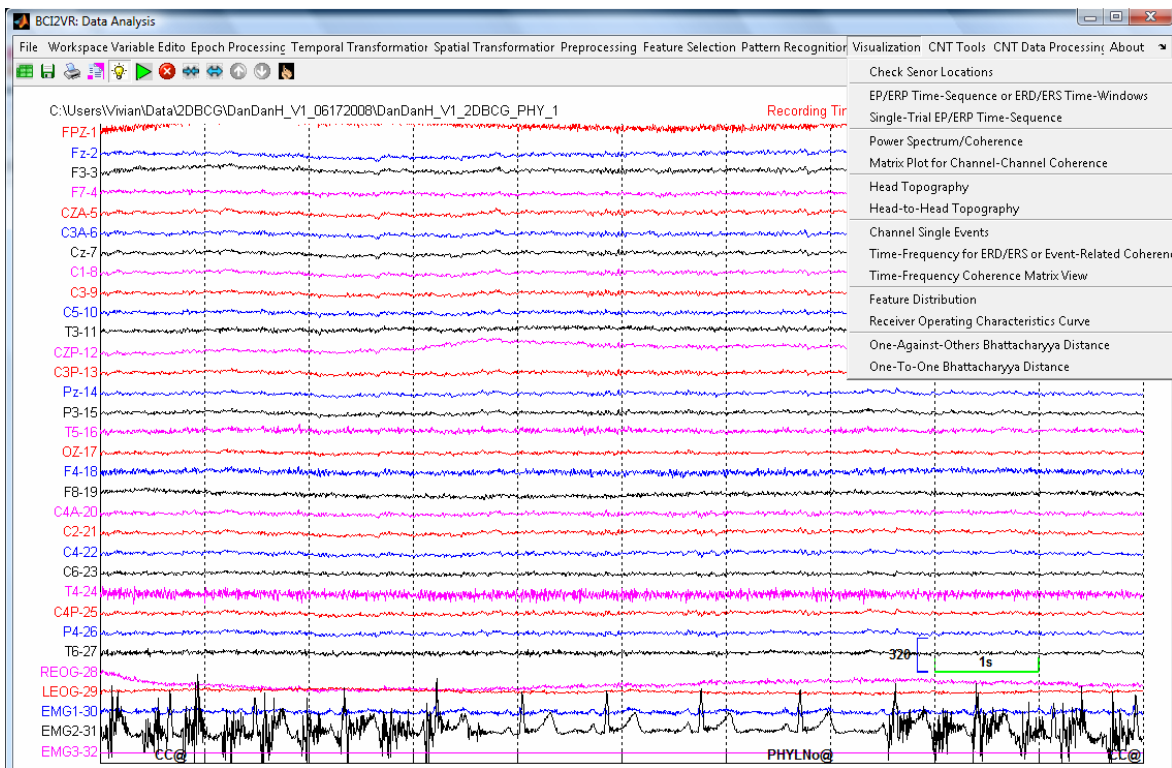
Figure 8. View continuous data in data analysis window: use menu bars or tool bars to change/scroll views.

21

CHAPTER 4

Computational Methods and Data Processing

Recent BCI studies reported that BCI performance in terms of both accuracy and efficiency can be further improved by applying advanced filters and more computationally intensive non-linear classification methods [38, 42]. We have employed simple linear methods first, and then more intensive computational methods have been explored to determine whether and how the classification performance could be further improved.

The online signal processing to decode movement intention consists of three steps: (1) spatial filtering, (2) temporal filtering, and (3) feature extraction and classification.

4.1 Spatial filtering

Surface Laplacian derivation (SLD) was applied. EEG signal from each electrode was referenced to the averaged potentials from the nearby four orthogonal electrodes [43]. SLD operation improves the localization of sources, by reducing the smearing effect in conducting layers of the head, and also reducing the common reference effect [44]. Besides, the EEG feature of local synchrony, i.e., frequency power changes, can be enhanced as well [45]. As a result, the spatial difference due to different hand movements might be more distinguishable.

22

4.2 Temporal filtering

Temporal filtering: the power spectral density was estimated from the spatially filtered EEG signal from the T2 window and according to the visual inspection of time-frequency plot of ERD and ERS (refer Results session and Figure 8 and 9), the time period 1s-2s after T2 window started was extracted in order to obtain the strongest ERD/ERS. Because the signal was no longer stationary or associated with certain motor task outside a short-lasting data window, the data length for estimation was limited so that the natural power estimation of ERD and ERS under the periodogram method was not a consistent estimation with a variance as large as the true spectrum. Welch method was applied with a Hamming window to reduce estimation variance and side-lobe effect [46]: the data in the selected time-window was segmented and periodograms from all segments were averaged to obtain smoothed estimation. The length of segment determining frequency resolution was compromised with the number of segments determining estimation variance so that segment length or frequency bin width needed to be optimized. The optimization was performed using cross-validation method with a Mahalanobis Linear Distance (MLD) classifier. We found 4 Hz frequency resolution or segment length of 256/4=64 under 50% overlapping, provided a better classification of ERD and ERS across subjects, which was consistent with what we used for binary control of 2D cursor movement [31].

4.3 Feature extraction and classification

For either physical movement or motor imagery, there were about 96 trials making the data pool of 96 samples with 16 samples for each of four classes. The offline performance of multi-class classification was evaluated from 10-fold cross-validation; 90% of data pool was used for training, and the other 10% was used for validation so that the validation dataset was independent from the training dataset. For classification methods using hyper-parameters or feature evaluation for feature selection, those parameters or features were also determined by training data set only. In the online game, the features for decoding the movement intention was extracted and classified using the parameters determined from the calibration dataset.

4.3.1 Feature extraction

Empirical feature reduction: assuming that movement intention associated cortical activities occur over the motor cortex, we reduced the channel number from 29 to 14, which covered both left and right motor area. Furthermore, as we did not expect relevant activities in the delta, theta and gamma band, only alpha and beta band (8-30Hz) activities were extracted for modeling and classification. Thus, the total number of extracted features were 8 (frequency bins) × 14 (channels) = 112 features.

Bhattacharyya distance: Bhattacharyya distance provides an index of feature separability for binary classification, which is proportional to the inter-class mean difference divided by intra-class variance [47]. The empirically extracted features were ranked by the Bhattacharyya distance for further classification.

Genetic algorithm: Genetic algorithm (GA)-based feature selection is a stochastic search in the feature space guided by the concept of inheriting, where at each search step, good properties of the parent subsets found in previous steps are inherited. 10-fold cross-validation was used with a Mahalanobis linear distance (MLD) classifier for feature evaluation [48]. In this approach, the population size we used was 20, the number of generations was 100, the crossover probability was 0.8, the mutation probability was 0.01, and the stall generation was 20.

4.3.2 Classification methods

Mahalanobis Linear Distance Classifier: Classification was done upon measuring Mahalanobis linear distance , which computed a pooled covariance matrix averaged from individual covariance matrices in all task conditions where the discriminant boundaries were hyper-planes leaning along the regressions [49]. All 112 features after empirical feature reduction were used for calculating the distance in high dimensional space.

GA-based Mahalanobis Linear Distance Classifier (GA-MLD): The sub-optimal feature subset was selected by GA, and the selected features providing the best cross-validation accuracy were applied to a Mahalanobis Linear Distance Classifier. The number of features for the subset was 4, which was determined from the cross-validation accuracy with feature numbers of 2, 4, 6, 8 and 10 from the calibration dataset of S1.

Decision Tree Classifier: Since a certain feature subset, for example, channels over the left motor cortex may be sensitive to discriminate the intention to move the right hand and

not sensitive for detecting other movement intentions, a decision tree method (DTC) was employed for the multi-class classification task in this study. At each level of DTC, the features for one-to-others classification were ranked by Bhattacharyya distance, and the 4 features with higher rank were used for classification by MLD. The number of the feature for classification was determined from preliminary comparison with numbers of 2, 4, 6, 8 and 10.

Support Vector Machine (SVM) Classifier: SVM tackles the principle of structure risk minimization with the consideration of maximization of the margin of separation [50]. As a consequence, SVM can provide a good generalization performance independent of the sample distribution. As a promising method, SVM has been suggested in a number of BCI applications [51, 52]. We employed a SVM approach provided in LIBSVM (Fan et al., 2005). The radial basis function was used as the SVM kernel function as it can provide similar classification outcome compared with other kernels [53]. As the performance of SVM depends on the regulation parameters or hyper-parameters C and the width of the kernel σ [54, 55], 10-fold cross-validation was performed; 2K , K from -5 to 15 with step of 2 for the penalty parameter and 2K, K from -15 to 5 with step of 2 for the spread parameter. These parameters were determined by the training dataset only.

4.4 Data processing for neurophysiological analysis

Offline data analysis was performed to investigate the neurophysiology following the tasks of 'Yes' and 'No' using the right or left hands. The calibration datasets were used for analysis. Data processing was performed using MATLAB Toolbox of BCI2VR. Epoching

26

was done with windows of -2s to 7s with respect to the first cue onset. Any epochs contaminated with artifacts were rejected. ERD and ERS were calculated for each case. Epochs were linearly de-trended and divided into 0.256s segments. The power spectrum of each segment was calculated using FFT with Hamming window resulting in a bandwidth of about 4 Hz. ERD and ERS were obtained by averaging the log power spectrum across epochs and baseline corrected with respect to -2s to 0s.

CHAPTER 5

Results of Neurophysiological Analysis

5.1 Neurophysiological analysis of ERD/ERS

The proposed BCI in this study intended to differentiate ERD and ERS patterns in two hemispheres following right hand and left hand movement or motor imagery. In the calibration session, for either hand, subjects performed motor execution or motor imagery during both T1 and T2 windows for the 'Yes' case, whereas they performed the same tasks during the T1 window and stopped to relax during T2 window for the 'No' case. The motor task was the same in T1 window for both 'Yes' case and 'No' cases. The spatiotemporal analysis following the 'No' cue onset was performed for either hand using the calibration dataset for both motor execution and motor imagery.

Figure 9 shows examples of time-frequency plots, head topographies of ERDs or ERSs for motor execution with physical movement, from Subject 1, 2, 3 and 4, respectively. For each subject, time-frequency plots of channel C3 over the left sensorimotor cortex and C4 over the right hemisphere are illustrated on the left two columns and head topography of ERD or ERS to their right, containing each of the four situations: 'RYes', 'RNo', 'LYes', and 'LNo'. In the time-frequency plot, 0 s stands for the first cue (green in the visual

paradigm) occurrence. ERD (blue color) was observed from around 0.5 - 1s after the cue onset due to the response delay; for S1, S2 and S3, ERD in both alpha and beta bands from 10-30 Hz was observed over motor areas contralateral to the hand moved. The ERS in red color was mainly observed in the beta band centered around 20 Hz over the contralateral motor areas. Compared with ERD patterns, ERS was short-lasting in time but highly distinguishable. The ERD and ERS topography shows beta band activity: 21-24 Hz for S1 and S2, and 17-20 Hz for S3. Therefore, the ERD and ERS on either left or right hemisphere provided four spatial patterns to detect 'RYes', 'RNo', 'LYes', and 'LNo' intentions. However, ERD and ERS were less distinguishable for S4 (21-24 Hz for topography).

Figure 10 shows the time-frequency plots and head topography of ERD and ERS associated with motor imagery. Similar to the patterns associated with physical movement, ERD associated with motor imagery was observed in both alpha and beta band on the contralateral hemisphere with the hand moved, although ERD amplitude was smaller than that of physical movement. ERS in the T2 window was observed on the contralateral hemisphere in beta band (13-24 Hz) only, and its amplitude was smaller than that of physical movement. During left hand motor imagery for S1 ('LYes'), ERD in T2 time window was also observed on the left hemisphere. The ERD and ERS associated with motor imagery also provided four spatially differentiable patterns, however, the smaller amplitudes of ERD and ERS with motor imagery may result less effective detection in single-trials.

(a)

30

(b)

31
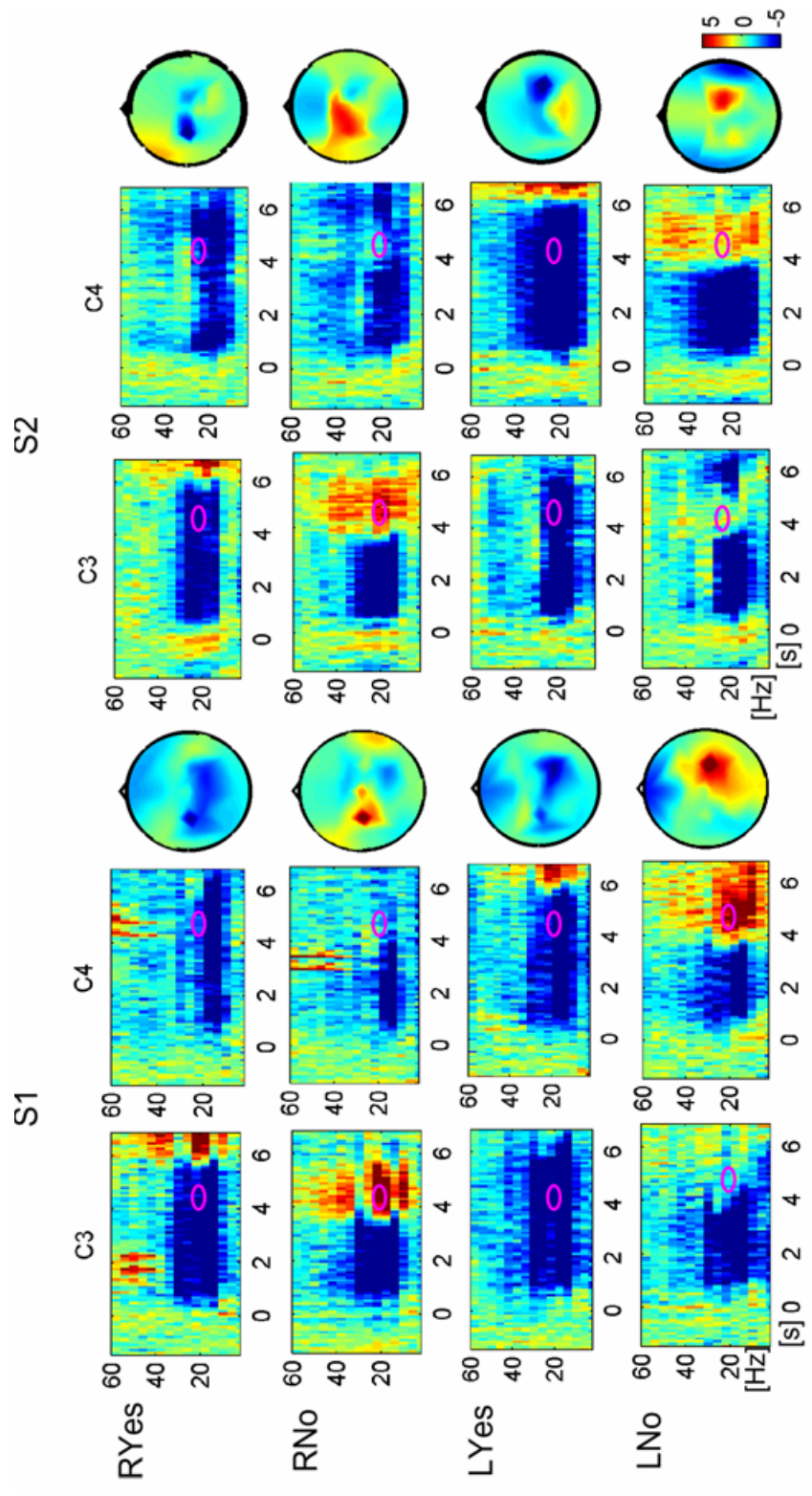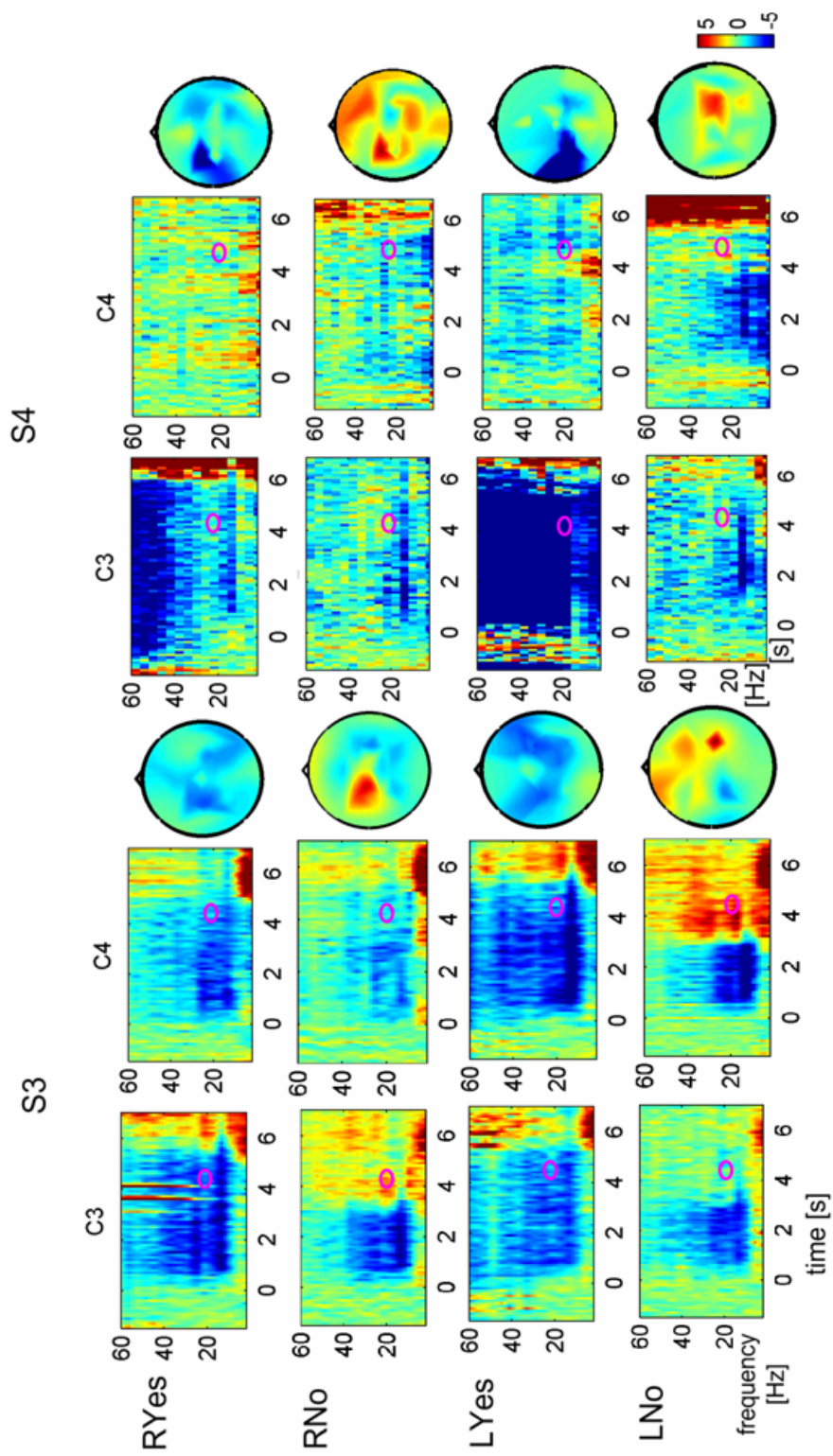
Figure 9. Time-course and topography of ERD and ERS during motor execution following calibration paradigm for S1, S2 (a), S3 and S4 (b). The horizontal coordinates are time in second and vertical coordinates are frequency in Hz for all the plots. The blue color stands for power decrease or ERD; the red stands for power increase or ERS. T1 window is from 0 s to 2.5s and T2 window from 2.5 s to 5 s. For S1, S2 and S3, ERD was observed in T2 window on left hemisphere during sustained right hand movement; ERS was observed in T2 window on left hemisphere when subjects ceased to move right hand movement. During left hand movement, ERD was observed in T2 window on right hemisphere during sustained movement and ERS on right hemisphere when subjects ceased to move left hand. ERD and ERS in each case were marked by pink circles in the time-course plot. The head topography corresponding to the pink marked time period was provided next to the time-course plots.

33

Figure 10. Time-couse and topography of ERD and ERS during motor imagery following calibration paradigm for S1 and S2. The horizontal coordinates are time in second and vertical coordinates are frequency in Hz for all the plots. For both S1 and S2, ERD is obtained in the time window with sustained motor imagery and ERS with termination of motor imagery. ERDs appear in both alpha and beta bands, bilateral, whereas ERSs appear only in alpha band on the contralateral hemisphere. ERD and ERS in each case were marked by pink circles in the time-course plot. The head topography corresponding to the pink marked time period was provided next to the time-course plots.

5.2 Feature analysis

The best frequency bands and channels for classifying movement intentions were determined from the calibration datasets. Figure 11 shows the spatial-frequency feature analysis indexed by Bhattacharyya distance for S1, S2, S3 and S4 during motor execution with physical movement, where all the channels over the whole head were used. The first column for each subject illustrates the channel-frequency plot of the Bhattacharyya distance, and the second column is the topography of the Bhattacharyya distance of the best frequency band. In Bhattacharyya distance plot, the dark red color shows the higher Bhattacharyya distance standing higher separability to classify movement intentions from single trial EEG signal.

Figure 11. Feature visualization indexed by Bhattacharyya distance for S1, S2, S3, and S4 during motor execution following the calibration paradigm. The best frequency band with the highest separability was found in beta band, and the best channel was found on sensorimotor areas.

In the channel-frequency plot for S1, the higher Bhattacharyya distance value for right hand physical movement was observed in beta band ranging from 17-24 Hz on the channels located on left hemisphere over the sensorimotor area. The high separability between ERD and ERS in beta band was consistent with the time-frequency analysis in Figure 9. The topography of the Bhattacharyya distance around 17-24 Hz shows that the best EEG spatial channels for the classification of 'RYes' and 'RNo' were in the contralateral left hemisphere over the sensorimotor area since ERS presented on contralateral left hemisphere only, although ERD occurred bilaterally as shown in Figure 9. A higher Bhattacharyya distance value for left hand physical movement was seen also in beta band on the contralateral right hemisphere. For S2, the distribution of Bhattacharyya distance values was similar to that of S1, except that for either right hand or left hand, 'Yes' case showed high separability only on contralateral hemisphere, which can be seen in the topography of Bhattacharyya distance. For S3, the best frequency band with the highest Bhattacharyya distance value was in the beta band around 13-24 Hz. The higher separability of beta band activity was consistent with the ERD and ERS features shown in Figure 9, where both ERD and ERS were seen only in beta band. For S4 with physical movement, the values of Bhattacharyya distance were much smaller than other subjects, although the spatial pattern was similar. The lower Bhattacharyya distance indicates that the classification would be much difficult from single trial signals.

Figure 12 shows feature analysis for S1 and S2 with motor imagery. For S1 and S2, distribution of higher Bhattacharyya distance values was similar to that with physical movement, but the separability was lower. The highest Bhattacharyya distance values were

38

in the beta band and on the channels over contralateral hemisphere for both right and left

hand motor imagery.

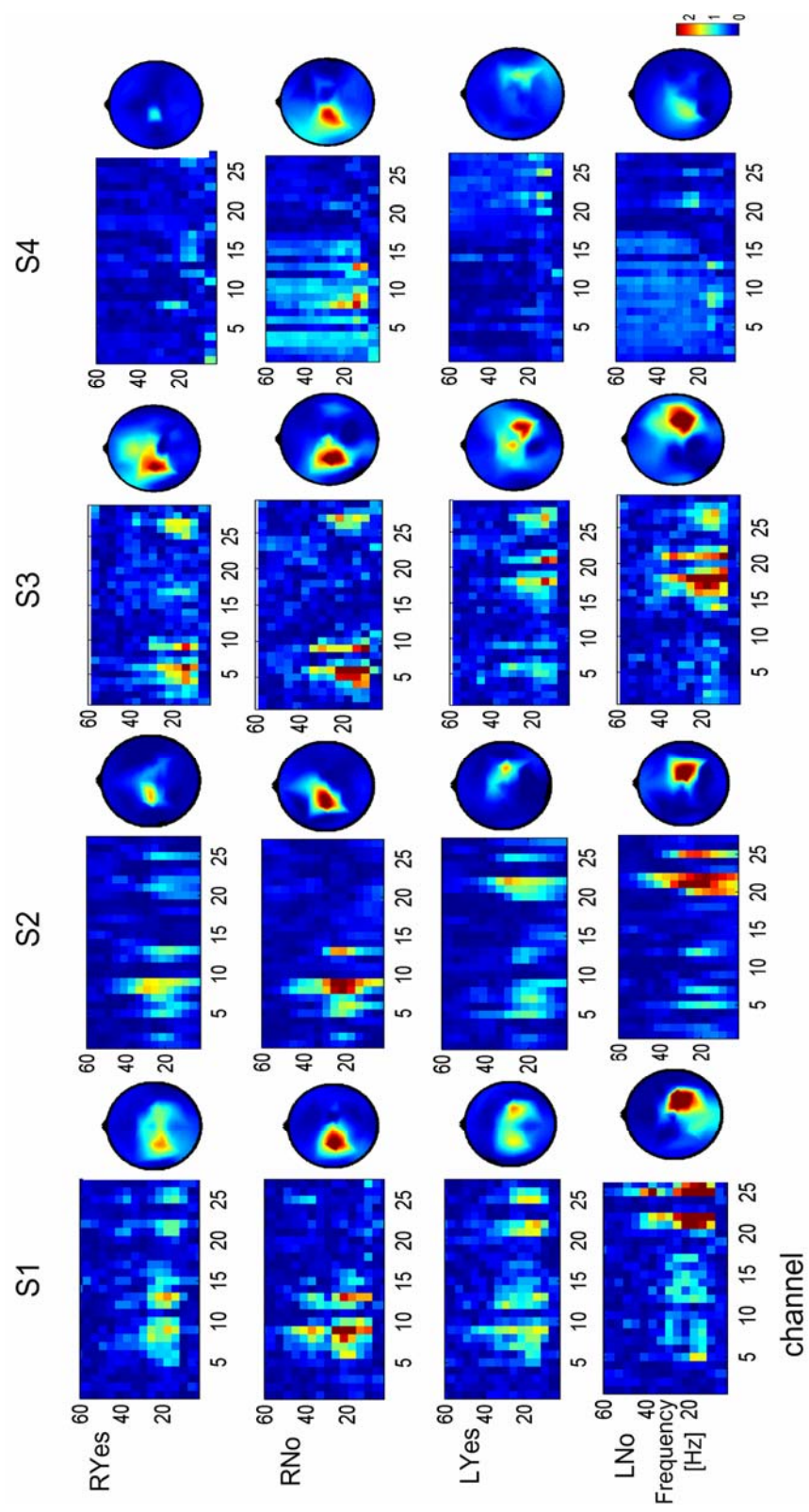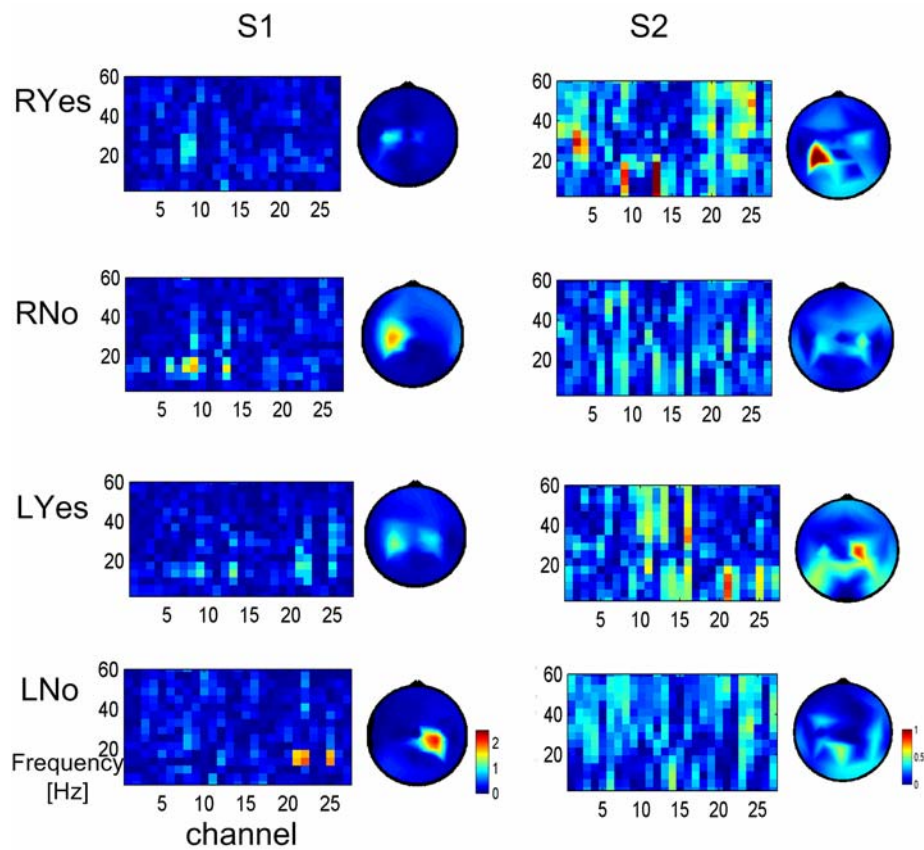**Figure 12. Feature visualization indexed by Bhattacharyya distance for S1 and S2 during motor imagery following the calibration paradigm. The horizontal coordinates are channel and vertical coordinates are frequency in Hz for all the plots. The best frequency band with the highest separability was found in beta band, and the best channel was found on sensorimotor areas.**

5.3 Classification

The comparison of 10-fold cross-validation accuracies using MLD, GA-MLD, DTC and SVM methods for S1, S2, S3 and S5 during physical movement is shown in Table 1. Since ERD and ERS patterns were not strong enough for S4, we excluded it from further exploration of classification methods. MLD has a mean value of 70.2%; after applying genetic algorithm in feature selection, GA-MLD provides an improved mean value of 88.3%. Using a paired t-test, GA-MLD is found to have a significant improvement of classification accuracy than MLD (t=7.64, df=3, p-value<0.01*). Similarly, we also compared DTC and SVM performance with that of MLD. Paired t-test gives the result showing that DTC outperforms MLD significantly (t=4.20, df=3, p-value<0.03*) and SVM improved significantly than MLD as well (t=5.56, df=3, p-value<0.02*).

Table 1. **10-fold Cross-Validation Accuracy**

Subject	MLD(%)	GA-MLD(%)	DTC(%)	SVM(%)
S1	63.1 ± 4.51	87.7 ± 1.29	87.8 ± 1.47	87.8 ± 1.31
S2	79.5 ± 6.21	93.0 ± 1.97	85.5 ± 3.87	90.0 ± 3.12
S3	67.3 ± 3.04	85.2 ± 0.95	84.5 ± 2.30	88.9 ± 1.04
S5	71.0 ± 2.18	87.2 ± 0.58	87.7 ± 1.75	85.8 ± 2.13
Average	70.2 ± 6.97	88.3 ± 3.33	86.4 ± 1.64	88.1 ± 1.79

MLD: Mahalanobis linear discrimination; GA-MLD: genetic algorithm-based

Mahalanobis linear discrimination; DTC: decision tree classifier; SVM: support vector

machine classifier

Although the intensive methods GA-MLD (mean 88.3%), DTC (mean 86.4%) and SVM (mean 88.1%) all performed better than MLD (mean 70.2%) significantly, there was no

significant difference among these three methods through one-way analysis of variance (AVONA), $F(1,2)=5.7$, p-value<0.39, alpha=0.05.

Since there was no significant difference among the intensive methods, DTC method was employed for the online 2D cursor control game. Except for S4, all the other four subjects were successful to control the cursor moving to the target by physical movement and the average online game performances for S1, S2, S3, and S5 were 92%, 85%, 81%, and 84%, with the overall performance of 85.5%±4.65%.

S1 and S2 participated in the second session performing motor imagery tasks. Offline classification accuracy for S1 was 73%±5.97%, and for S2 was 59.2%±3.63%, which were lower than those of physical movement with physical movement. The two subjects both reported good concentration throughout the recording, except that S2 felt sleepy in a short period in the middle. Online 2D cursor control game using motor imagery was performed by S1 and S2. S1 was able to move the cursor to the target; However, S2 performed less well than S1. The performance was consistent with the classification results for motor imagery.

CHAPTER 6

Discussion and Future Directions

6.1 Spatial detection of ERD/ERS

We observed contralateral ERD and ERS in the beta band during sustained movements and post movement from all subjects when they performed physical movements; ERD over the motor area on left hemisphere associated with sustained right hand extension; post-movement ERS or beta band rebound occurring when stopping movement; ERD on right hemisphere associated with sustained left hand extension and ERS with cessation of the movement. ERD and ERS patterns on left and right hemispheres were highly differentiable for subjects S1, S2, S3 and S5, whereas it was less detectable for S4. For motor imagery, S1 and S2 showed similar ERD/ERS patterns as those with physical movement. The amplitudes of ERD/ERS, however, were smaller. Although the ERD/ERS patterns were expected to be similar between physical movement and motor imagery, we considered that the effectiveness of motor imagery, i.e. how to vividly imagine limb movement, might highly affect cortical ERD/ERS patterns.

The reason for the fact that motor imagery has less robust performance than physical movement might be that motor imagery is not a natural behavior and thus requires more

effort than performing physical movement. Besides, compared with physical movement, there is no neural feedback in motor imagery which may exhibit less activity (ERS) in motor cortex and result in lower signal to noise ratio. Considering that motor imagery is more meaningful for BCI application, training may be needed to enhance the involvement of subjects with motor imagery.

6.2 Decoding rate and accuracy

The BCI performance can be evaluated from both the decoding rate and accuracy [1]. Wolpaw et al. introduced the information transfer rate (ITR) for a BCI as bits per minute (bpm) as a good measurement for both decoding rate and accuracy [6]. In our study of 2D control, accuracies for physical movement ranged from 85.2% to 93.0% (given by GA-MLD, although not significantly better than DTC and SVM), with the average 88.3%; for a four-class mental task, ITR was from 1.16 bits per trial, to 1.37 bits per trial, with the average 1.29 bits per trial. For motor execution with physical movement, the total duration of T1 and T2 windows was 5 s, i.e. 12 trials per minute. Therefore, the ITR was 13.9 to 16.5; the average was 15.5 bits per minute. Similarly, for motor imagery, the ITR was 4.15 bits per minutes to 8.03 bits per minutes. The cuing period T1 is important as it left enough time for the subjects to prepare for the movement. The results were comparable in terms of both accuracy and decoding rate with previous studies (see review in [1]). We consider that the T1 window can be further shortened or optimized when subjects can make rapid

response, and as a result, the ITR can be further improved. We also consider that the control performance/accuracy is very important in practical BCI application. As BCI is intended for patients having limited motor function which features extremely slowness in motor control, it may be appropriate to have limited communication speed, whereas the accuracy needs to be high enough so that the users may avoid frustration when using BCI.

Invasive methods using spike train or local field potentials [12, 22], or at least semi-invasive method using ECoG [19], have been investigated as the major signal methods for two-dimensional (or three dimensional) BCI control. The noninvasive signal method, though more convenient for practical application, has been less studied. This study provides further evidence for two-dimensional BCI control using noninvasive method. From spatial detection of ERD and ERS, two-dimensional control was reliable with detection accuracy of 80-90%.

In conventional 2D BCI cursor control paradigm, the target locations were at four margins in 2D monitor [25]. We proposed a new BCI paradigm, in which the target may be at any place in 2D monitor. On the other hand, the previous 2D control was achieved by accurate control of EEG frequency power so that long-term training was required before subject was able to regulate EEG rhythm precisely. In the current proposed BCI methods, BCI cursor control was achieved by the ERD and ERS associated with natural motor behavior so that long-term training was no longer required.

6.3 Difficulty and improvement

Unlike in binary motor imagery [32] where subjects imagine the movement of only one limb of the body, motor imagery in 2D motor control tasks can be more difficult, since subjects need to respond quickly to each imagery task and switch reactions successfully among the four tasks. Fatigue is a common issue during data collection, which requires a relatively long time and repetitive motor tasks. To maximize subject involvement so that they are highly motivated, the paradigm can be further improved in terms of a better design and a shorter calibration time, which will greatly benefit BCI application. Also, the subjects can be trained more as to how to avoid fatigue in the experiments. These issues will be considered and addressed in the subsequent studies.

6.4 Possible contamination of muscle artifact

EMG contamination from facial muscles may possibly cause serious problems in BCI development [56]. Throughout the experiment, EMG signal was monitored for all subjects, to make sure correct movements were performed and no EMG occurred during motor imagery. Further, the signal for classification was extracted from around 3.5s-4.5s with respect to the first color cue onset (i.e. 1s-2s after T2 started) so that the artifact contaminated signal outside this period was not included; feature analysis showed that beta activities restricted to motor areas were used for classification. Therefore, the EMG contamination was not a concern in this study.

6.5 Classification method analysis

Mahalanobis Linear Distance uses a large number of features for classification. In multi-class classification tasks, a very large data set is used for proper training, and further, a feature subset may perform well for some classes but poorly for others. 'DTC' has been employed for overcoming these difficulties, to use multi-level classification under the 'divide and conquer' principle. Support vector machine (SVM) approach also provides good control of model complexity to avoid over-fitting, but due to the requirement for determining hyper-parameters, the training time in offline modeling might be longer. Furthermore, the determining hyper-parameters may need a larger sample set. Taking into all these considerations, 'DTC' would be preferable for online 2D cursor control, since it has good performance and is simple and fast.

6.6 Implications of proposed BCI

BCI has been proposed for patients who may lose voluntary muscle contraction. In the extreme state such as in patients with amyotrophic lateral sclerosis (ALS), individuals may be entirely 'locked-in' though their cognition is still intact. Under these conditions, BCI is then only possible with motor imagery. The two-dimensional BCI control in this study shows that reliability or accuracy was less with motor imagery than with physical movement. However, only two subjects have been studied with motor imagery so that further study with more subjects should be addressed. For patients who are not in a 'locked-in' state but cannot produce reliable muscle contraction due to muscle weakness or

spasticity, we would expect more reliable two-dimensional control with their limited motor output as this study demonstrates a highly reliable control with simple physical movement.

BCI has been proposed as an interface to control external devices directly from the brain for the purpose of restoring motor function. Recently, another potential application of BCI has been recognized, as a tool to augment brain plasticity and outcomes for neurological rehabilitation. i.e. BCI could be employed for the rehabilitation of motor and cognitive impairments in hemiplegic or paraplegic patients by offering on-line feedback about cortical activity associated with mental practice, motor intention, and other neural recruitment strategies during progressive task-oriented practice [57].

In this study, the set up time for electrodes over whole scalp was around 15-20 minutes. As this is an exploration study, we applied electrodes over the whole scalp. From the feature analysis in Figure 11, we found that the electrodes over motor cortex provided better features for classification. Therefore, the number of electrodes for future practical application can be further reduced and electrode setup time might be reduced to within 10 minutes.

In summary, ERD/ERS using our 2D natural paradigm present four distinguishable patterns as we expected, both in physical movement and imagery. Although variability might lead to considerable challenges in the classification process, the intensive methods we applied exhibit satisfying properties and robust results, making 2D control more reliable. It is worthwhile to pursue this potential system since EEG is less expensive, flexible, and has established analysis techniques. If the design and signal processing methods can be further improved, BCI products will eventually offer those who have

totally lost muscle control with convenient, fast and reliable control of mechanical devices. This will largely reduce the reliance on continuous support from others, and thus enhance their quality of life.

Literature Cited

Literature Cited

1.　Wolpaw, J.R., et al., *Brain-computer interfaces for communication and control.* Clin Neurophysiol, 2002. **113**(6): p. 767-91.

2.　Vaughan, T.M., J.R. Wolpaw, and E. Donchin, *EEG-based communication: prospects and problems.* IEEE Trans Rehabil Eng, 1996. **4**(4): p. 425-30.

3.　Birbaumer, N., A.R. Murguialday, and L. Cohen, *Brain-computer interface in paralysis.* Curr Opin Neurol, 2008. **21**(6): p. 634-8.

4.　Hinterberger, T., et al., *Brain-computer communication and slow cortical potentials.* IEEE Trans Biomed Eng, 2004. **51**(6): p. 1011-8.

5.　Wolpaw, J.R., et al., *An EEG-based brain-computer interface for cursor control.* Electroencephalogr Clin Neurophysiol, 1991. **78**(3): p. 252-9.

6.　Wolpaw, J.R., et al., *Brain-computer interface technology: a review of the first international meeting.* IEEE Trans Rehabil Eng, 2000. **8**(2): p. 164-73.

7.　Gao, X., et al., *A BCI-based environmental controller for the motion-disabled.* IEEE Trans Neural Syst Rehabil Eng, 2003. **11**(2): p. 137-40.

8.　Muller-Putz, G.R., et al., *EEG-based neuroprosthesis control: a step towards clinical practice.* Neurosci Lett, 2005. **382**(1-2): p. 169-74.

9.　Anderson, J.R., et al., *An integrated theory of the mind.* Psychol Rev, 2004. **111**(4): p. 1036-60.

10. Wolpaw, J.R., *Adaptive plasticity in the spinal stretch reflex: an accessible substrate of memory?* Cell Mol Neurobiol, 1985. **5**(1-2): p. 147-65.

11. Moss, A.H., et al., *Patients with amyotrophic lateral sclerosis receiving long-term mechanical ventilation. Advance care planning and outcomes.* Chest, 1996. **110**(1): p. 249-55.

12. Carmena, J.M., et al., *Learning to control a brain-machine interface for reaching and grasping by primates.* PLoS Biol, 2003. **1**(2): p. E42.

13. Scherberger, H., M.R. Jarvis, and R.A. Andersen, *Cortical local field potential encodes movement intentions in the posterior parietal cortex.* Neuron, 2005. **46**(2): p. 347-54.

14. Wolpaw, J.R. and D.J. McFarland, *Multichannel EEG-based brain-computer communication.* Electroencephalogr Clin Neurophysiol, 1994. **90**(6): p. 444-9.

15. Kauhanen, L., et al., *EEG and MEG brain-computer interface for tetraplegic patients.* IEEE Trans Neural Syst Rehabil Eng, 2006. **14**(2): p. 190-3.

16. LaConte, S.M., S.J. Peltier, and X.P. Hu, *Real-time fMRI using brain-state classification.* Hum Brain Mapp, 2007. **28**(10): p. 1033-44.

17. Coyle, S., et al., *On the suitability of near-infrared (NIR) systems for next-generation brain-computer interfaces.* Physiol Meas, 2004. **25**(4): p. 815-22.

18. Sitaram, R., et al., *Temporal classification of multichannel near-infrared spectroscopy signals of motor imagery for developing a brain-computer interface.* Neuroimage, 2007. **34**(4): p. 1416-27.

19.   Schalk, G., et al., *Two-dimensional movement control using electrocorticographic signals in humans.* J Neural Eng, 2008. **5**(1): p. 75-84.

20.   Andersen, R.A., S. Musallam, and B. Pesaran, *Selecting the signals for a brain-machine interface.* Curr Opin Neurobiol, 2004. **14**(6): p. 720-6.

21.   Lebedev, M.A. and M.A. Nicolelis, *Brain-machine interfaces: past, present and future.* Trends Neurosci, 2006. **29**(9): p. 536-46.

22.   Donoghue, J.P., *Connecting cortex to machines: recent advances in brain interfaces.* Nat Neurosci, 2002. **5 Suppl**: p. 1085-8.

23.   Birbaumer, N. and L.G. Cohen, *Brain-computer interfaces: communication and restoration of movement in paralysis.* J Physiol, 2007. **579**(Pt 3): p. 621-36.

24.   Soyuer, F., et al., *The relationship between fatigue and depression, and event-related potentials in epileptics.* Epilepsy Behav, 2006. **8**(3): p. 581-7.

25.   Wolpaw, J.R. and D.J. McFarland, *Control of a two-dimensional movement signal by a noninvasive brain-computer interface in humans.* Proc Natl Acad Sci U S A, 2004. **101**(51): p. 17849-54.

26.   Birbaumer, N., *Brain-computer-interface research: coming of age.* Clin Neurophysiol, 2006. **117**(3): p. 479-83.

27.   Leeb, R., et al., *Brain-computer communication: motivation, aim, and impact of exploring a virtual apartment.* IEEE Trans Neural Syst Rehabil Eng, 2007. **15**(4): p. 473-82.

28.   Jarosiewicz, B., et al., *Functional network reorganization during learning in a brain-computer interface paradigm.* Proc Natl Acad Sci U S A, 2008. **105**(49): p. 19486-91.

29.   Krusienski, D.J., et al., *A mu-rhythm matched filter for continuous control of a brain-computer interface.* IEEE Trans Biomed Eng, 2007. **54**(2): p. 273-80.

30.   McFarland, D.J. and J.R. Wolpaw, *EEG-based communication and control: speed-accuracy relationships.* Appl Psychophysiol Biofeedback, 2003. **28**(3): p. 217-31.

31.   Bai, O., et al., *Exploration of computational methods for classification of movement intention during human voluntary movement from single trial EEG.* Clin Neurophysiol, 2007. **118**(12): p. 2637-55.

32.   Bai, O., et al., *A high performance sensorimotor beta rhythm-based brain-computer interface associated with human natural motor behavior.* J Neural Eng, 2008. **5**(1): p. 24-35.

33.   Bai, O., et al., *Asymmetric spatiotemporal patterns of event-related desynchronization preceding voluntary sequential finger movements: a high-resolution EEG study.* Clin Neurophysiol, 2005. **116**(5): p. 1213-21.

34.   Rao, S.M., et al., *Functional magnetic resonance imaging of complex human movements.* Neurology, 1993. **43**(11): p. 2311-8.

35.   Stancak, A., Jr. and G. Pfurtscheller, *Event-related desynchronisation of central beta-rhythms during brisk and slow self-paced finger movements of dominant and nondominant hand.* Brain Res Cogn Brain Res, 1996. **4**(3): p. 171-83.

36.   Pfurtscheller, G. and T. Solis-Escalante, *Could the beta rebound in the EEG be suitable to realize a "brain switch"?* Clin Neurophysiol, 2009. **120**(1): p. 24-9.

37.   Neuper, C., et al., *Imagery of motor actions: differential effects of kinesthetic and visual-motor mode of imagery in single-trial EEG.* Brain Res Cogn Brain Res, 2005. **25**(3): p. 668-77.

38.   Naeem, M., et al., *Seperability of four-class motor imagery data using independent components analysis.* J Neural Eng, 2006. **3**(3): p. 208-16.

39.   Oldfield, R.C., *The assessment and analysis of handedness: the Edinburgh inventory.* Neuropsychologia, 1971. **9**(1): p. 97-113.

40.   Neuper, C., et al., *Motor imagery and action observation: modulation of sensorimotor brain rhythms during mental control of a brain-computer interface.* Clin Neurophysiol, 2009. **120**(2): p. 239-47.

41.   Jasper, H.H. and H.L. Andrews, *Electro-encephalography. III. Normal differentiation of occipital and precentral regions in man.* Arch Neurol Psychiat, 1938. **39**: p. 95-115.

42.   Muller-Gerking, J., G. Pfurtscheller, and H. Flyvbjerg, *Designing optimal spatial filters for single-trial EEG classification in a movement task.* Clin Neurophysiol, 1999. **110**(5): p. 787-98.

43.   Hjorth, B., *An on-line transformation of EEG scalp potentials into orthogonal source derivations.* Electroencephalogr Clin Neurophysiol, 1975. **39**(5): p. 526-30.

44.   Nunez, P.L., et al., *EEG coherency. I: Statistics, reference electrode, volume conduction, Laplacians, cortical imaging, and interpretation at multiple scales.* Electroencephalogr Clin Neurophysiol, 1997. **103**(5): p. 499-515.

45.   Pfurtscheller, G., *Mapping of event-related desynchronization and type of derivation.* Electroencephalogr Clin Neurophysiol, 1988. **70**(2): p. 190-3.

46.   Welch, P.D., *The Use of Fast Fourier Transform for the Estimation of Power Spectra: A Method Based on Time Averaging Over Short, Modified Periodograms.* IEEE Trans. Audio Electroacoust., 1967. **AU-15**: p. 70-73.

47.   Chatterjee, A., et al., *A brain-computer interface with vibrotactile biofeedback for haptic information.* J Neuroeng Rehabil, 2007. **4**: p. 40.

48.   Li, Q. and K. Doi, *Analysis and minimization of overtraining effect in rule-based classifiers for computer-aided diagnosis.* Med Phys, 2006. **33**(2): p. 320-8.

49.   Marques, J.P., *Pattern recognition: concepts, methods and applications*. 2001, Berlin: Springer-Verlag.

50.   Vapnik, V. and O. Chapelle, *Bounds on error expectation for support vector machines.* Neural Comput, 2000. **12**(9): p. 2013-36.

51.   Olson, B.P., et al., *Closed-loop cortical control of direction using support vector machines.* IEEE Trans Neural Syst Rehabil Eng, 2005. **13**(1): p. 72-80.

52.   Thulasidas, M., C. Guan, and J. Wu, *Robust classification of EEG signal for brain-computer interface.* IEEE Trans Neural Syst Rehabil Eng, 2006. **14**(1): p. 24-9.

53.   Keerthi, S.S. and C. Lin, *Asymptotic behaviors of support vector machines with Gaussian kernel.* Neural Computation, 2003. **15**(7): p. 1667-89.

54. Muller, K.R., et al., *An introduction to kernel-based learning algorithms.* IEEE Trans Neural Netw, 2001. **12**(2): p. 181-201.

55. Chang, C.C. and C.J. Lin, *Training nu-support vector classifiers: theory and algorithms.* Neural Comput, 2001. **13**(9): p. 2119-47.

56. McFarland, D.J., et al., *Brain-computer interface (BCI) operation: signal and noise during early training sessions.* Clin Neurophysiol, 2005. **116**(1): p. 56-62.

57. Dobkin, B.H., *Brain-computer interface technology as a tool to augment plasticity and outcomes for neurological rehabilitation.* J Physiol, 2007. **579**(Pt 3): p. 637-42.

58. Rodriguez-Rivera, A., B.D. Van Veen, and R.T. Wakai, *Statistical performance analysis of signal variance-based dipole models for MEG/EEG source localization and detection.* IEEE Trans Biomed Eng, 2003. **50**(2): p. 137-49.

59. Babiloni, F., et al., *Multimodal integration of high-resolution EEG and functional magnetic resonance imaging data: a simulation study.* Neuroimage, 2003. **19**(1): p. 1-15.

60. Mitra, P.P. and B. Pesaran, *Analysis of dynamic brain imaging data.* Biophys J, 1999. **76**(2): p. 691-708.

61. Percival, D.B. and A.T. Walden, *Spectral Analysis for Physical Applications: Multitaper and Conventional Univariate Techniques*. 1993, Cambridge: Cambridge University Press.

62. Huan, N.J. and R. Palaniappan, *Neural network classification of autoregressive features from electroencephalogram signals for brain-computer interface design.* J Neural Eng, 2004. **1**(3): p. 142-50.

63.   Raymer, M.L., et al., *Dimensionality reduction using genetic algorithms.* Evolutionary Computation, IEEE Transactions on, 2000. **4**(2): p. 164-71.

64.   Li, J., et al., *An efficient feature selection algorithm for computer-aided polyp detection.* International Journal on Artificial Intelligence Tools, 2006. **15**(6): p. 893-915.

65.   Garrett, D., et al., *Comparison of linear, nonlinear, and feature selection methods for EEG signal classification.* IEEE Trans Neural Syst Rehabil Eng, 2003. **11**(2): p. 141-4.

66.   Hung, C.I., et al., *Recognition of motor imagery electroencephalography using independent component analysis and machine classifiers.* Ann Biomed Eng, 2005. **33**(8): p. 1053-70.

67.   Lal, T.N., et al., *Support vector channel selection in BCI.* IEEE Trans Biomed Eng, 2004. **51**(6): p. 1003-10.

68.   Erfanian, A. and B. Mahmoudi, *Real-time ocular artifact suppression using recurrent neural network for electro-encephalogram based brain-computer interface.* Med Biol Eng Comput, 2005. **43**(2): p. 296-305.

APPENDIX A

Filtering

A.1. Spatial filtering

The spatial filter applies a transformation matrix that is determined under certain constraints to the EEG signal so that the filtered signal may have a better signal-to-noise ratio for identifying the changes of the underlying neuronal sources. This procedure is similar to beamforming, which can increase the gain in the direction of the task-related signals and decrease the gain in the direction of interference and noise[58]. As a result, the spatial filter may improve classification accuracy. The signal from electrodes was directly fed into the temporal filter.

'SLD' performs surface Laplacian transformation on multi-dimensional EEG signals. Realistic Laplacian transformation usually requires a head shape model, which can be constructed from brain imaging [59]. We employed a simple method, which is also called a 'reference-free' method so that the signal is independent of which electrode is used as reference. The EEG signal from each electrode was referenced to the averaged potentials from four orthogonal nearby electrodes. SLD operation enhanced the spatial resolution of local EEG potentials by reducing the volume conduction effect. SLD applies a high-pass filter to suppress low-spatial frequency components along with volume conduction components so that the local synchronizations, in particular, their radial components, have

increased spatial specificity [45] and as a result, the spatial difference following hand movements might be more discriminable.

A.2. Temporal filtering

Two temporal filtering methods were explored. The temporal filters were performed on spatially filtered EEG trials. The signal power obtained from temporal filters was represented in logarithmic form. 'VAR' calculated the variance of the spatial filtered signal, i.e., whole frequency band power of the signal.

'PSD' estimated power spectral densities of the spatial filtered signal using the Welch method. A Hamming window was employed to reduce side lobe effect. The FFT length was set to $0.256\,\mathrm{s}$ resulting in a frequency resolution of approximately $4\,\mathrm{Hz}$. Power spectral densities were smoothed from segments with 50% overlapping. A number of PSD estimation methods have been used in the signal processing literature, each of which varies in resolution and variance of the estimation. Periodogram or modified periodogram has higher spectral resolution, but the resulting variance is also larger than that of the Welch method [46]. The multitaper method provides a solution to balance the variance and resolution [60]. However, an optimal multitaper method permits the trade-off between resolution and variance to usually be data-dependent [61]. We did not employ parametric methods, for example, using autoregressive model coefficients [62]. The parametric model requires determining model order. Further, the model coefficients for classification are also indirect to frequencies, which are difficult for general neurophysiological analysis.

59

APPENDIX B

Feature preprocessing

Features having large variances may dominate the learning process in the classifier training. The filtered data (features) were scaled to zero mean and unit standard deviation of one for numeric stabilization.

APPENDIX C

Feature selection

The spatially and temporally filtered EEG signals provided high-dimensional features; for example, 27 EEG channels with 16 frequency bins produced 432 features. Because of the noisy nature of EEG, such high-dimensional features may bias the classification model producing a low testing accuracy. A compact subset of features needs to be determined for achieving a robust classification. The subset feature selection can be determined either empirically or 'data-driven'. Because of the high dependence among features, the empirical approach usually does not provide a good solution. The exhaustive search method is one of the optimal feature selection methods, which evaluates all possible subsets to determine the best subsets. For example, the exhaustive search of a subset of 3 features from 432 features results in more than ten million combinations. It is impractical to perform this due to the computational burden. We adopted a sub-optimal method of genetic algorithm-based search, which is a stochastic search in the feature space guided by the idea of inheriting, at each search step, good properties of the parent subsets found in previous steps [63]. One important procedure in the genetic algorithm-based feature selection is the evaluation of feature subsets. In this study, the feature subsets were evaluated on 10-fold cross-validation accuracy using a Linear Mahalanobis Distance

61

(LMD) classifier in order to reduce the risk of over-training [64]. According to the evaluation of the feature subset, a new generation was created from the best of them. By repeating this procedure, a sub-optimal feature subset for the classification was determined. In this approach, the dimension of feature subset should be provided previously. We performed a pilot study to investigate an optimal dimension. Because of the difference in spatial and temporal filters, it was difficult to determine an optimal dimension. We proposed the strategy of grid search from 4 to 20 with step of 4 according to the finding in the pilot study. In GA approach, the population size was 20, the number of generations was 100, the crossover probability was 0.8, the mutation probability was 0.01, and the stall generation was 20.

Because of the large number of features, the convergence speed under GA was still very slow. For the purpose of faster convergence and less risk of local minima, we proposed an approach of pre-feature selection to pre-select features having larger Bhattacharyya distance between two task conditions. The Bhattacharyya distance is the square of mean difference between two task conditions divided by the variance of the samples in two task conditions [49]. The Bhattacharyya distance was calculated on each feature (univariate) in feature pool indexing the feature separability between two task conditions, which was somewhat similar to ANOVA statistic test by evaluating the volume of the pooled covariance matrix of the class relative to the separation of their means. As Bhattacharyya distance indexes the separability directly, it is preferable for feature selection with comparison of other indexing methods, for example, the Fisher Score which indexes the

similarity. The features were sorted in descending order according to their Bhattacharyya distance; the first 100 features were retained for subsequent multivariate feature selection.

APPENDIX D

Classification

We explored three statistical classification and three neural network classification approaches. For pattern recognition, the simplest classification can be achieved by finding the minimum distance to the prototypes, usually the sample means under different tasks. For example, in the case of a two-feature two-class classification problem, the discriminant boundary is a straight line perpendicular to the linking of means and passing at half distance. Because the features are not necessarily mutually uncorrelated, we adopted linear and quadratic Mahalanobis distance, which takes covariance into account [49]. 'LMD' computed a pooled covariance matrix averaged from individual covariance matrices in two task conditions so that the discriminant boundary is hyper-planes leaning along the regression.

We explored a nonlinear classification approach using neural networks. The neural network approaches provide more complicated discriminant boundaries, for example, by using polynomial functions. Theoretically, it may provide higher accuracy in classification tasks, at least in the training procedure. Successful applications in BCI development have also been reported ([65] and [66]).

Support vector machines (SVM) tackle the principle of structure risk minimization with the consideration of maximization of the margin of separation [50]. As a consequence, SVM can provide a good generalization performance independent of the sample distribution. As a promising method, SVM has been suggested in a number of BCI applications ([67], [51] and [52]). We employed a SVM approach provided in LIBSVM [68]. We selected the RBF as the kernel function since the RBF kernel can provide a similar classification outcome compared with other kernels [53]. Two data-dependent parameters needed to be determined in the training procedure; the penalty parameter for controlling model complexity and the spread parameter for RBF functions. A 2-D grid searching with 5-fold cross-validation was performed; 2^K, K from -5 to 15 with step of 2 for the penalty parameter and 2^K, K from -15 to 5 with step of 2 for the spread parameter.

APPENDIX E

Experimental Procedure

The following steps were taken during every experiment.

Before the subject comes, the following steps should be done:

1. Turn on power 1 & 2 of the amplifiers.

2. Restart PC.

3. Check control panel: make sure USB is recognized.

4. EEG device calibration:

   Start BCI2VR shortcut on the desktop ->

   Select Data Acquisition from the pump-up bar ->

   File->load set-up file -> (C: SharedFolder->BCI2VR_Toolbox->setup_files-
   >g32ChwholeHead_btv_daq_settings.m) double click. ->

   Run calibration (the green button 'C') and wait->

   Check the values in command window, all should be close to '1'. Accept it.

When subject comes:

5. Electrodes setup (placement of EEG channels, EMG, and EOG can be referred in
   method part)-> connected to the amplifiers

6. Check Impedances: click the blue button 'I' in Data Acquisition interface. If impedances are low enough which are shown in blue, then close the window.

7. Start recording:

    Click the green triangle button to show waveform.->

    And then open 'Target Stimuli' from the bar. Drag the window to the right screen->

    File-> load stim file (C: SharedFolder->BCI2VR_Toolbox->application->2DCursorControl->calibration_stim.m)->

    (This step is needed for the first time: Run it for a while, let the subject be familiar with the paradigm.)-> stop it.->

8. From the Acquisition interface, choose the button next to the green triangle, recording data. ->

    Input a daq name for this dataset.

    (First build a new folder for this subject in:

    C: Sharedfolder ->New_EEG_data.

    Name the new folder like DandanH_V2_08192008.

    Open this folder and give a name for the new dataset. Like

    DandanH_V2_2DBCG_phy_1 or img or mix compared to phy. 1 stands for the first

    dataset for physical movement.

    Then click save.)

    See the waveform, wait until steady.

    From the Target Stimuli window, select 'run',

and click 'Edit' to change the mode to either '1'- phy or '2'-img or '3'-mix.

Remind the subject to focus on the screen, and then click on the black background.

Move the mouse to the left screen. The recording starts!

9   11 minutes later the stimuli stopped. So the conductor close it by clicking the red

button. And also stop the recording in Data Acquisition interface.

The results are shown.

10 Start recording the second dataset: repeat step 8 & 9.

----

11 After two datasets for phy, play the game:

From the Target stimuli, load a new file(C: Sharedfolder->BCI2VR_Toolbox-

>application->2DCursorControl->2DBCG_stim.m)-> Edit->numberofDataFile:2

or 4, phy or mix.

Open a new file(2DCursorControl->recalibration.m), change parameters when

needed. Run it.

Record the waveform-> give it a name like DandanH_V2_game_1.

Wait until steady. -> play the game.

12 Record two datasets for img. Not necessary to play the game.

13 Record 4 for mixed movements, and repeat step 11.

14 After finishing all the recording, take all the electrodes off the subject and provide

him/her with towel and shampoo to clean. Conductor will need to shut down the

amplifiers, clean electrodes and cap, take down all necessary results and make

another copy of the data.

VITA

Dandan Huang was born in November 1984, in Tianjin, China. She got her Bachelor of Engineering degree in 2007 with the major of Biomedical Engineering at Tianjin University in China. In fall 2007, she continued her study in Biomedical Engineering at Virginia Commonwealth University, where she worked as a research assistant, and was invited to be a member in Phi Kappa Phi Honor Society, AEMB Biomedical Engineering Honor Society and IEEE society. Currently she is pursuing a Master's degree with the thesis research related with brain-computer interface.